

Wearable postural control system for low back pain therapy

Alvaro Rodriguez, Juan R. Rabuñal, *Member, IEEE*, Alejandro Pazos *Member, IEEE*, Antonio Rodríguez Sotillo and Norberto Ezquerra

Abstract—Treatment of low back pain usually includes exercise, analgesics, prostheses, and in severe cases, surgery. Early treatments based on postural control are essential to prevent low back pain and mitigate permanent damage.

We present a wearable device, with an estimated cost below 100\$, that uses inertial units with tri-axial accelerometers, gyroscopes and magnetometers to measure the orientation of three sections of the spine. The device integrates the absolute and relative orientation from the sensors to estimate the posture of the back in real time and uses a fuzzy system to control a vibration unit that indicates the user when to correct the posture of the back.

We validated the device in controlled conditions, obtaining an RMS Deviation $\leq 1.24^\circ$, and conducted a preliminary clinical pilot study with patients afflicted by *lumbar hyperlordosis* or *lumbar hypolordosis*. We observed an improved postural control and a reduction of low back pain in all cases. These results show a promising potential of the device to reduce pain, improve postural therapies and raise postural awareness in patients affected with low back pain.

Index Terms— Back orientation; Inertial Measurement Unit; Fuzzy System; Low back pain; Posture therapy.

I. INTRODUCTION

LOW back pain is one of the most common reasons people go to the doctor or miss work, and it is a leading cause of disability worldwide [1]. More than 80% of the population have low back pain at least once [2].

We define low back pain as muscle tension, stiffness or other general pain localized below the costal margin and above the inferior gluteal folds, with or without leg pain (sciatica).

A study in the United States found that, of all patients with low back pain in primary care: 4% have a compression fracture, 3% spondylolisthesis, 0.7% a tumor or metastasis, 0.3% ankylosing spondylitis, 0.01% an infection [3], and around 90% have non-specific low back pain, which in essence, is a diagnosis based on exclusion of specific pathology [4].

First submitted to IEEE Transactions on Instrumentation and Measurement on August 2020. This research received funding from the European Regional Development Fund (FEDER) and the Instituto de Salud Carlos III, under grant agreement PI17/01826. This project has also received funding from the General Directorate of Culture, Education and University Management of Xunta de Galicia under grant agreements ED431D 2017/16 and ED431C 2018/49; the Drug Discovery Galician Network under grant agreement ED431G/01 and the Galician Network for Colorectal Cancer Research under grant agreement ED431D 2017/23. The Spanish Ministry of Innovation and Science, through the CYTED Network under grant agreement PCI2018-093284. Finally, the European Regional Development Fund (FEDER) and the Spanish Ministry of Economy and Competitiveness have supported this project through the funding of the unique installation BIOCAI under grant agreements UNLC08-1E-002 and UNLC13-13-3503.

The most important symptoms of non-specific low back pain are pain and disability [4], commonly attributed to muscle or ligament strains caused by repeated heavy lifting or sudden awkward movements. Moreover, prolonged mechanical stresses on the spine resulting from occupational activities, are important causes of non-specific low back pain [1]. Low back pain is also related to many conditions of abnormal curvatures in the spine such as *scoliosis* (sideways curve in the spine), *lumbar hyperlordosis* (excessive extension of the lumbar region), *lumbar hypolordosis* (abnormally straight or even flexed lumbar region) or *thoracic hyperkyphosis* (excessive convex curvature in the thoracic and sacral regions).

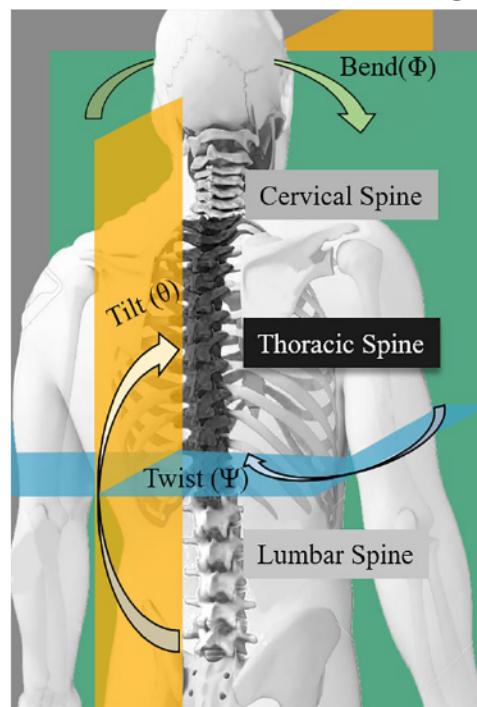


Fig. 1. Spine sections and angular motions.

Alvaro Rodriguez is with the Department of Computer Science of the University of A Coruña, Spain and the Biomedical Research Institute of A Coruña (INIBIC), A Coruña, Spain. (Correspondence address: Faculty of Informatics, University of A Coruña, Campus Elviña s/n 15071; phone: +34981167000; e-mail: a.tajes@udc.es).

Juan R. Rabuñal is with the Department of Computer Science, University of A Coruña, Spain and the Center for Technological Innovation in Construction and Civil Engineering (CITEEC), A Coruña, Spain.

Alejandro Pazos is with the Department of Computer Science of the University of A Coruña, Spain and the Biomedical Research Institute of A Coruña (INIBIC), A Coruña, Spain.

Antonio Rodríguez Sotillo is with the Spinal Cord Injury Unit, University Hospital Complex, A Coruña, Spain.

Norberto Ezquerra is with Nortec LLC, Atlanta, USA.

Treatments to low back pain include opioid medications, spinal injections, and in the worst cases, prostheses and surgery [2]. Nonetheless, the most common treatments in the first line of action, or as components of a broader package, are Spinal Manipulative Therapies (SMT) and exercise regimes [5]. Moreover, experimental results indicate that exercise in combination with education is likely to reduce the risk of low back pain [6], and clinicians recommend improving posture, general fitness, achieving a healthy weight, or paying attention to posture as the most effective strategies for the prevention of low back pain [7].

Postural control and maintenance of postural stability are therefore, essential capacities in daily life, and can be major factors when preventing low back injuries or improving the efficiency of exercise therapies. These therapies require accurate proprioceptive information and functional motor control in the trunk and lower limbs to achieve appropriate muscular responses [8]. However, low back pain patients often have these capacities affected, as they exhibit a reduced variability in postural control strategies due to a decreased proprioceptive reweighting capacity that is associated with a decreased postural robustness [9].

To increase postural awareness in low back pain patients, and to improve their ability of self-supervision during therapy exercises, our device measures the posture of the patients, and informs them when a correction is necessary.

Posture monitoring systems have been used in previous works for supporting orthopedic rehabilitation [10], performance monitoring in combat sports [11], monitoring postural stability [12], measuring balance control [13], therapy instruction and correction [14], posture classification [15], measuring standing inclination motion [16], trunk posture monitoring [17] and many other applications. These systems were also applied in the topic of this research with applications in spine conditions such as: *scoliosis* and *hyperkyphosis* [18], *scoliosis* [19] and rehabilitation after back spine surgery [20].

The technology used in these previous works includes: inductive sensors [21], [22], camera or optical systems [23]–[25], tracking suits [26], [27], accelerometers [19], [28], [29], or Inertial Measurement Units (IMUs) [10]–[20]. Inductive sensors measure changes in length and are not suitable to measure back rotations and angles that are necessary in our research; optical systems and tracking suits are usually expensive and require specific facilities; and devices based on accelerometers only, are affected by drift and not reliable enough for mid-long sessions. Thus, in our opinion, IMU technology is currently the best suited for this work.

Previous IMUs systems monitored the back in different ways. Thus, configurations with one [12], [13], two [16], [19], [20] and three sensors [15], [17], [18] are common in the literature. According to [30], five sensors placed at equal distances are necessary to reconstruct the spine shape. However, five-sensor configurations are impractical to wear, expensive and no other work we are aware of uses this configuration. Advised by clinicians, we consider that a three-sensor configuration, with sensors placed in the upper trunk (T1/T2), middle trunk (T12) and pelvis (S1), is the most effective solution to monitor conditions such as *scoliosis*, *lumbar hyperlordosis*, *lumbar hypolordosis* and *thoracic hyperkyphosis*; where the spine can acquire a s-shape curvature, and therefore cannot be observed with less than 3 sensors. This configuration was successfully used to study some of these problems in [17], [18].

Comparing our device with the previous IMU devices for posture monitoring applicable in our scenario [15]–[20]. They didn't present accuracy results with real back motions [15], [19], [20], present lower accuracy [16]–[18]; and were not tested with real patients [15]–[20].

In addition to posture monitoring, our device detects when the position of the back deviates from predefined parameters, and informs

the user in real time on when to correct the posture using a vibrotactile system. This approach was tested with success in applications such as preventing excessive walking sway [31] detection of loss of balance in hospital and home-care patients [32], optimization of training exercises [33] and in rehabilitation environments [14], [34]; but has not been used before in conjunction with posture monitoring sensors to assist low back pain patients with postural therapy

The device works as follows. First, the clinician establishes the correct biomechanical position (baseline posture) for the activity; and uses the provided software to define permitted deviation for each angular movement and section of the column. The baseline posture and permitted deviation are specific to each user and activity. And we defined them based on information extracted from physiotherapy sessions, such as the range of motions each patient was able to perform.

When the user wears the device and performs the programmed activity. The device uses the three IMUs, each one composed by an accelerometer, a gyroscope and a tri-axial magnetometer, to obtain postural measurements in real time. If the posture deviates from the baseline, a fuzzy expert system controls a vibration unit that sends a stimulus to the user to correct the posture when appropriate.

The device records the performance of the user in each training session, so the user and the clinician can extract the data and review the session, observing the evolution of correct and incorrect postures with their timestamps in a graphic interface. This information is vital to adapt therapies and activities to each person, and to define and improve exercise plans.

To our knowledge, the only commercial alternatives to perform a similar functions have a price range of 2000\$–4000\$, and do not provide technical details or an accuracy comparison [35]–[37]. The estimated cost of our solution, if commercialized, is below 100\$.

In summary, our device is a cost effective wearable that measures the posture of the back in real time using 3 IMU units; and then uses a feedback system controlled by a fuzzy expert system to give information back to the user. As far as our knowledge goes, this is the first time this strategy is used to assist low back pain patients with postural therapy; and the first time a postural control system reports results with low back pain patients.

II. MATERIALS AND METHODS

A. Measuring the angular movements of the spine

The spinal column, also called vertebral column, starts at the base of the skull and continues to the pelvis. It contains layers of bone called vertebrae, and cartilaginous discs that absorb and distribute the pressure and prevent friction during movement.

The spine contains three segments that form three natural curves when viewed from the side. Two "c-shaped" curves in the neck and lower back, called *lordosis*, conform the cervical and lumbar spine segments. They have 7 and 5 vertebrae respectively. Between them, one "reverse c-shaped" curve called *kyphosis* forms the thoracic spine segment with 12 vertebrae.

We describe the posture of the spinal column with three angular motions: *Bend* defined as the rotation in the front-to-back or longitudinal axis, *X*; *Tilt*, that represents the rotation around the transverse or *Y*-axis of the body; and *Twist*, which represents the rotation within the horizontal plane, i.e. the vertical or *Z*-axis of the body. Fig. 1 shows the spine rotations in detail.

To measure the angular motions of the spine, we integrate three orthogonal gyroscopes that measure the angular velocity, three accelerometers that measure the acceleration and three magnetometers that calculate the orientation using the magnetic field of the Earth.

These sensors present primarily two sources of error. First, there is a noise component or bias, which affects the three gyroscopes and

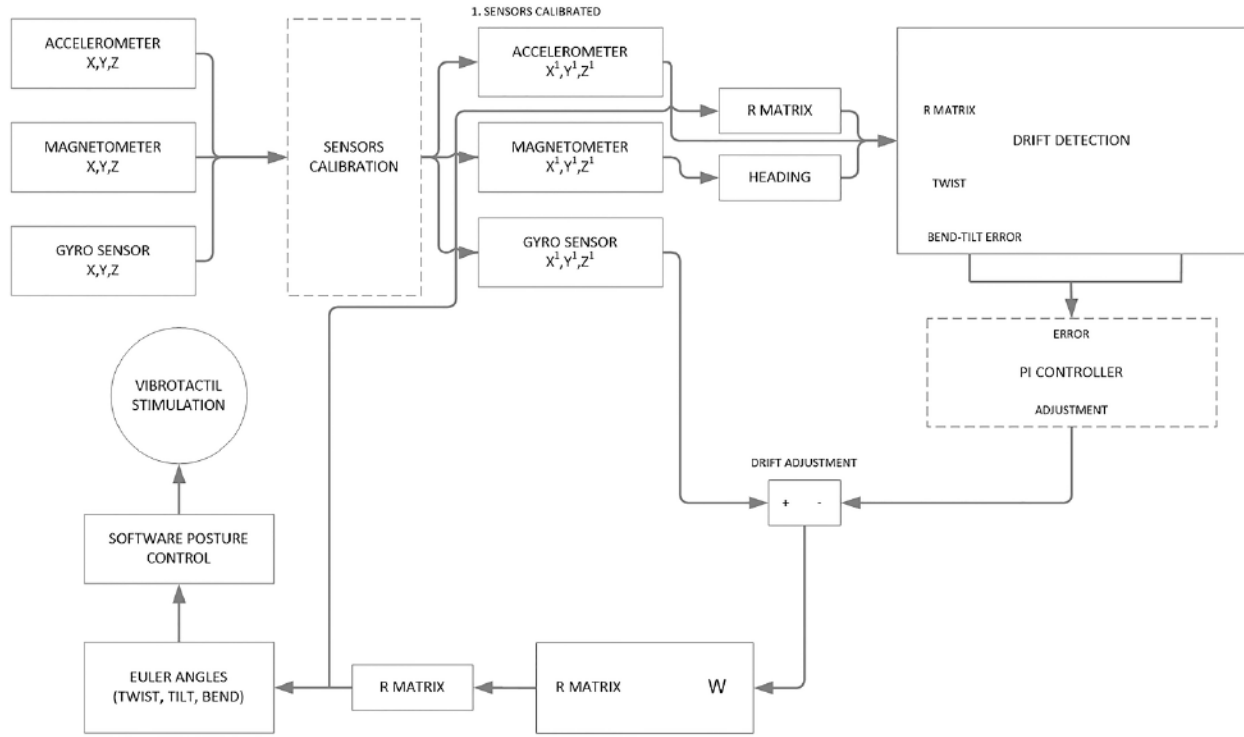


Fig. 2. Scheme implementation of the DCM algorithm in the postural control device.

accelerometers. We remove this source of error subtracting the average signal registered in a long term analysis with the device in a resting position with no rotation [38], [39]. The second source of error is the tendency of the signal to drift out from the initial position. Drift is one of the biggest problems of gyroscopes. We correct the drift in the gyroscopes using the information from the accelerometers and magnetometers.

After the error correction, we integrate all the nine sensors to obtain the rotation matrices that describe the relative position of the spine with respect to the coordinate system of the Earth in the upper trunk, middle trunk and pelvis, and in relation to each other.

From the Earth frame of reference, the R_x , R_y and R_z transformations represent the rotations of the spine in the position of the sensor with their corresponding rotation angles: *Bend* (ϕ), *Tilt* (θ), and *Twist* (ψ).

Eq. (1) shows the equation to rotate a vector measured in the frame of reference of the spine to the frame of reference of the Earth [40]:

$$\begin{bmatrix} u_x \\ u_y \\ u_z \end{bmatrix} = R_z R_y R_x \begin{bmatrix} v_x \\ v_y \\ v_z \end{bmatrix} = R \begin{bmatrix} v_x \\ v_y \\ v_z \end{bmatrix} = \begin{bmatrix} r_{xx} & r_{xy} & r_{xz} \\ r_{yx} & r_{yy} & r_{yz} \\ r_{zx} & r_{zy} & r_{zz} \end{bmatrix} \begin{bmatrix} v_x \\ v_y \\ v_z \end{bmatrix} \quad (1)$$

$$\begin{aligned} r_{xx} &= \cos \theta \cos \psi \\ r_{xy} &= \sin \phi \sin \theta \cos \psi - \cos \phi \sin \psi \\ r_{xz} &= \cos \phi \sin \theta \cos \psi + \sin \phi \sin \psi \\ r_{yx} &= \cos \theta \sin \psi \\ r_{yy} &= \sin \phi \sin \theta \sin \psi + \cos \phi \cos \psi \\ r_{yz} &= \cos \phi \sin \theta \sin \psi - \sin \phi \cos \psi \\ r_{zx} &= -\sin \phi \\ r_{zy} &= \sin \phi \cos \theta \\ r_{zz} &= \cos \phi \cos \theta \end{aligned}$$

Being u_x, u_y, u_z a vector in the frame reference of the Earth, and v_x, v_y, v_z a vector in the frame reference of the spine. The R matrix, also called Direction Cosine Matrix (DCM) [41], is updated from the gyroscopic signals according to Eq. (2) [41].

$$R(t+dt) = R(t) \begin{bmatrix} 1 & -w_z(t)dt & w_y(t)dt \\ w_z(t)dt & 1 & -w_x(t)dt \\ -w_y(t)dt & w_x(t)dt & 1 \end{bmatrix} \quad (2)$$

Being $w(t)$ the rotation rate measured by the gyroscopes in the corresponding axis. However, as gyroscopes are not reliable enough to measure positions in long periods due to its drift. We add in Eq. (3) a correction term.

$$w(t) = w_{gyro}(t) + w_{correction}(t) \quad (3)$$

Eq. (4) represents the *Twist* correction vectors using the magnetometers [40].

$$\text{Correction}_{Twist} = R^T \begin{bmatrix} 0 \\ 0 \\ r_{xx}y_c - r_{yx}x_c \end{bmatrix}$$

$$\begin{aligned} x_c &= x_{mag} \cos(\theta) - z_{mag} \sin(\theta) \\ y_c &= y_{mag} \cos(\phi) + z_{mag} \sin(\phi) \end{aligned} \quad (4)$$

Being $x_{mag}, y_{mag}, z_{mag}$ the output of the magnetometers and, x_c, y_c, z_c the corrected values. However, despite *Twist* correction being common, is still the bottleneck in the accuracy of IMUs. As magnetometers are sensitive to magnetic interference caused by metal objects close to the subject. In our scenario, we take advantage of having 3 separated magnetometers to reduce the short term effect of this interference by using the mobile average of the magnetometers.

Also, as magnetic interferences should be similar in all sensors and the orientation of the back is determined by relative displacements, instead of absolute ones. We also included a function to sync periodically the magnetometers when the 3 sensors are aligned in the same orientation and plane, setting their 0 position. This feature increases the long term reliability of the output.

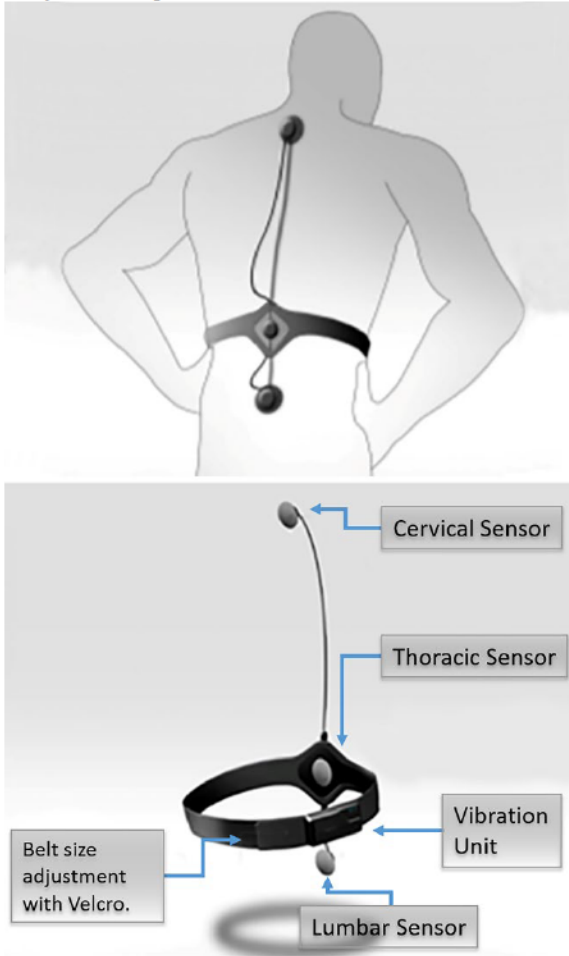


Fig. 3. Postural control device. The IMU are sensors placed in the upper trunk (T1/T2), middle trunk (T12) and pelvis (S1). Each sensor is attached to the skin using a surface adhesive electrode with a snap button.

Eq. (5) shows the *Tilt-Bend* correction vectors using the accelerometers [40].

$$Correction_{Tilt-Bend} = \begin{bmatrix} r_{zx} \\ r_{zy} \\ r_{zz} \end{bmatrix} \times \begin{bmatrix} x_{acc} \\ y_{acc} \\ z_{acc} \end{bmatrix} \quad (5)$$

Being x_{acc} , y_{acc} , z_{acc} the output of the accelerometers, and r_{zx} , r_{zy} , r_{zz} the Z row of the direct cosine matrix.

After obtaining the *Twist* and *Tilt-Bend* correction vectors, we feed them to a proportional Plus Integral (PI) feedback controller, which output $w_{correction}$, is the additive correction term to the gyroscopes from Eq. (3) that allow us to update the *R* matrix. Eq. (6) shows the equation of the PI controller.

$$w_{correction}(t) = K_p e(t) + K_I \int_{\tau=0}^t e(\tau) d\tau$$

$$e(t) = W_{Twist} Correction_{Twist}(t) + W_{Tilt-Bend} Correction_{Tilt-Bend}(t) \quad (6)$$

Being K_p and K_I constant tuning parameters called proportional and integral gain tuned using the Ziegler–Nichols method [42]; $e(t)$ the estimation error in moment t ; and W_{Twist} and $W_{Tilt-Bend}$ weight parameters adjusted empirically to provide a rapid response (large weighting) to *Twist* relative to *Tilt* and *Bend* [41].

Finally, after updating the DCM matrix, the Euler angles that describe the orientation of the back can be obtained from the *R* matrix, using Eq. (7) [40]:

$$\begin{aligned} \psi &= \arctan(r_{yx}, r_{xx}) \\ \theta &= -\arcsin(r_{zx}) \\ \phi &= \arctan(r_{zy}, r_{zz}) \end{aligned} \quad (7)$$

Fig. 2 details the implementation of the DCM algorithm.

B. Architecture and design

The device consists of a belt with three IMUs sensors located in the cervical, thoracic and lumbar areas and were attached to the skin using a surface adhesive electrode with a snap button (Fig. 3). Each IMU sensor measures the displacements in the X, Y and Z-axis in a section of the spine. Each IMU uses an ADXL345 gravitational 3-axis accelerometer with up to 13-bit resolution at ± 16 g, maintaining 4 mg/LSB scale factor in all g ranges; an ITG3200 3-axis gyroscope with a sensitivity of 14.375 LSBs per $^{\circ}/\text{sec}$ and a full-scale range of $\pm 2000^{\circ}/\text{sec}$; and a HMC5883 3-axis magnetometer with up to 1° in compass heading accuracy.

For the vibration unit, we used a common coin shaped 12000 rpm mobile phone vibration motor.

The device also contains a 16 MHz ATmega 328P processor that receives the data obtained by the IMUs, obtaining the inclination, curvature and rotation of the back in real time.

An additional 16 MHz ATmega 2560 processor controls the Bluetooth and USB communication interfaces, activates or deactivates the vibration unit to stimulate the user reaction, and records the data in a micro SD card, all in real time. Finally, we also included a set of physical buttons to control the main functions of the device.

The normal operation frequency of the device is measurements per second.

C. Fuzzy control system

The device has three internal states that determine the vibration response in real time:

- State 0: The posture is correct. The variable t_d (deactivation time) measures how long the position of the back has been inside the specified parameters, and resets when transitioning to this state.
- State 1: The posture is incorrect. When the device reaches this state from the State 0, the variable t_a (activation time) resets and counts the time the posture of the back deviates from the specified parameters.
- State 2: The posture is incorrect, and the vibration unit activates.

Fig. 4 shows a schematic with the states, transitions and variables that define the responses of the device. The control rules of the expert system in the device are as follows:

- In State 0, when the device detects an incorrect posture, it goes immediately to State 1.
- In State 1 or State 2, the device goes instantly to State 0 when the position of the back returns to the specified parameters.
- If the device stays in State 1 for some time (t_a reaches a threshold $t1$), it will enter State 2 and activate the vibration unit.
- Unless the device remains in State 0 for some time (t_d reaches a threshold $t2$), $t1$ is set to 0.

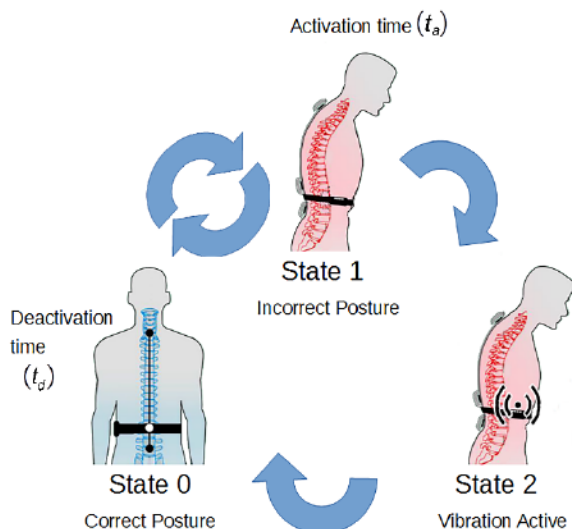


Fig. 4. States, transitions and time variables of the device.

We added a fuzzy logic to the device to obtain a more flexible and natural behavior. According to it, when the back is in a correct position for a long time, it takes longer to vibrate after the detection of an incorrect posture. In addition, if the posture is correct for a shorter time, it takes less time to vibrate. The time base thresholds for the device are currently established by the clinician, using time ranges from 10 to 25 seconds, to allow for a non-intrusive feedback over long periods of times.

In summary, we created a fuzzy system to control the vibration response of the device. This system contains an expert system based in a small set on rules, and a fuzzy strategy to prevent the vibration response unit from activating or deactivating during sudden movements in daily activities. Thus, fuzzy sets define the thresholds of the system $t1$ and $t2$ using initial reference values provided by the clinician.

The time thresholds and the baseline posture are, thus, configuration parameters of the system that can be tuned individually. This patient-based approach allows clinicians to plan individual training sessions, and to adjust movement ranges and speed responses to the goals of the session and to the patient. The clinician or the patient, after a supervised training period, can then gradually lower these parameters as the posture improves.

III. EXPERIMENTAL RESULTS

A. Static validation

To validate the accuracy of the device when measuring static orientations. We fixed the device at predefined rotation angles and, using a pendulum that we graduated with marks for each degree of amplitude. We performed 50 measurements at random orientations, using different sensors and rotation axis, ranging from -45 to 45 degrees.

The RMS error for the experiment was in all cases $< 1^\circ$, with an average value of 0.54° and a maximum error of 0.80° .

B. Dynamic Validation with a Rocking Platform

To validate the accuracy when measuring angular motions. We fixed the device to a rocking platform with a programmable periodic oscillating movement, and compared the oscillations measured by the IMUs with the ground truth obtained with an optical system [43], [44].

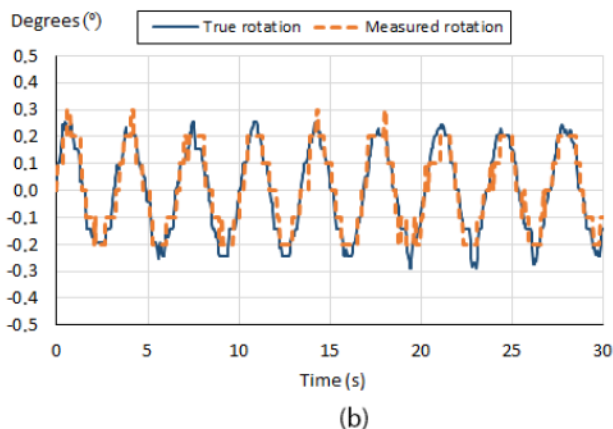
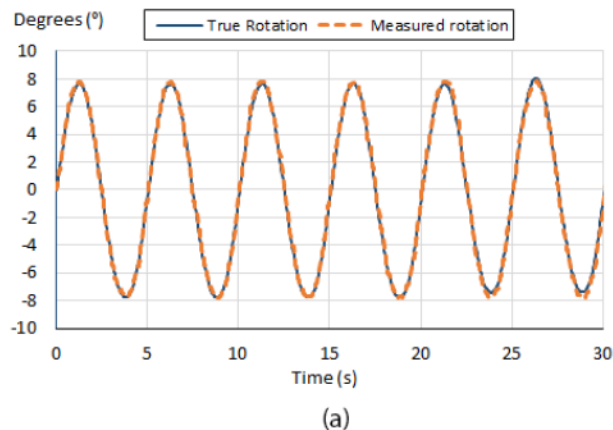


Fig. 5. Tilt rotation measured by the device and ground truth for the experiments with the rocking platform. (a) Experiment with 15° of amplitude and a frequency of 0.2Hz . (b) Experiment of 0.5° of amplitude and a frequency of 0.3Hz . Bend and twist rotations present identical results.

We conducted the rocker experiments with oscillation amplitudes of 15° and 0.5° for all axis, obtaining an almost identical accuracy in the *Bend*, *Tilt* and *Twist* measurements of the IMU. The maximum error was of 0.22° for the movements of 15° , and of 0.05° for the movements of 0.5° , showing a very good performance in all cases.

Table I and Table II show the average and maximum measurement errors for each axis, and Fig. 5 details the results for *Tilt* as an example.

TABLE I
AVERAGE ERROR ($^\circ$)

Axis (Rotation)	AVERAGE ERROR ($^\circ$)	
	0.5° Experiment	15° Experiment
X (Bend)	0.03	0.17
Y (Tilt)	0.04	0.15
Z (Twist)	0.05	0.16

TABLE II
MAXIMUM ERROR ($^\circ$)

Axis (Rotation)	MAXIMUM ERROR ($^\circ$)	
	0.5° Experiment	15° Experiment
X (Bend)	0.09	0.20
Y (Tilt)	0.14	0.20
Z (Twist)	0.15	0.22

C. Dynamic Validation with Back Exercises

We designed an experiment to validate the device in real conditions, in the back of a real person when performing a back exercise.

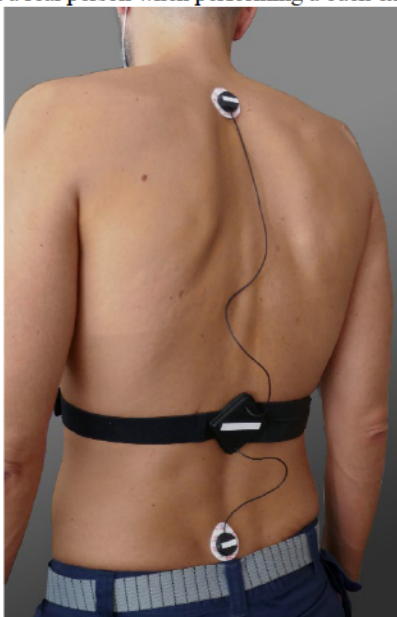


Fig. 6. One of our lab members wearing the device moments after one of the exercise sessions in the validation experiment.

The experiment consisted in performing a series of lateral bending exercises starting from a neutral upright sitting position, using different speeds and amplitudes of movement. And comparing the measurements of the device with the ones provided by an optical system.

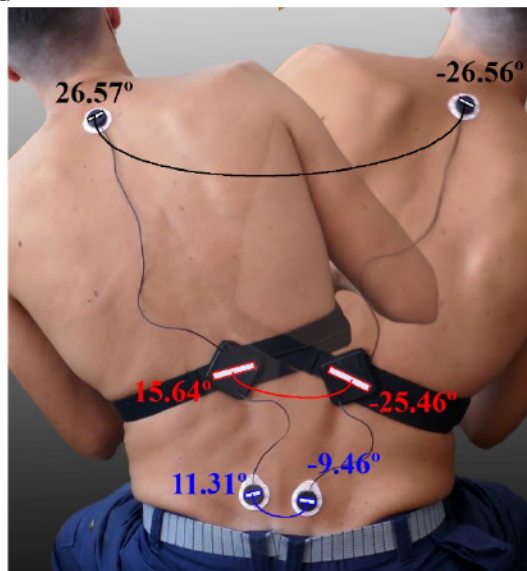


Fig. 7. Exercise session in the validation experiment. The figure represents a composite image from two frames in one of the recorded videos. Colored rectangles show the detected position of the markers by the computer vision algorithm, and next to each marker is displayed the corresponding orientation estimated by the algorithm.

It should be noted that we assumed that the performance of the sensors will be similar in all planes, as supported by sensor specifications, our previous results and previous works. This was also assumed in all similar experiments in the literature [16]–[18].

The optical system we used for reference consisted on a set of white

rectangular stick markers placed in each sensor, a video camera to record the experiments and a computer vision algorithm implemented in *OpenCv* to analyze the images.

We used a Panasonic DMC-TZ101 camera, placed in parallel to the bending plane at a distance of 1,2 meters, and recorded the experiment in Full-HD resolution at 50 frames per second using a tripod and manual focus configuration. The computer vision algorithm tracked the markers in the image using contrast difference and the *OpenCv* implementation of the Douglas-Peucker algorithm for polygonal shape fitting [45]. The results of this algorithm were latter verified using a block-matching technique to measure subpixel displacements in deformable surfaces published in [46], [47] obtaining a maximum difference of 0.4° and no significant average difference for the two algorithms.

The validation process consisted in comparing the change in the orientation of the markers registered by the optical system, with the change in orientation in each sensor registered by the device.

Fig. 6 shows one of our lab members wearing the device for the experiment and Fig. 7 illustrates the operation of the Computer Vision algorithm during the experiment.

We performed 3 recordings, with 3 to 5 series of exercises per recording, and each recording lasted approximately 5 minutes. Fig. 8 shows an example of the rotation obtained with the device, and the corresponding estimation from the optical system during one of the exercises.

To minimize the evaluation error, we focused our numerical comparison on the thoracic sensor and the lumbar sensor, as during the exercises, the plane of the cervical sensor with respect to the camera plane was not stable enough to obtain useful readings from the camera. In addition, to estimate the RMS difference between the optical system and the device, we manually aligned the output signals of both systems and we used bilinear interpolation to be able to compare the same timestamps.

The average RMS deviation for these experiments was $\leq 1.24^\circ$, and the maximum absolute obtained error was 6.34° . Despite the RMS deviation being probably overestimated due to the contribution of interpolation and alignment error sources. These results are comparable to or better than the ones in similar experiments [16]–[18], where the authors reported the average RMS deviation between the their sensor modules and a 3-D video-based motion analysis system with six cameras (Vicon 370, Oxford) for single plane motions. Table III shows these results.

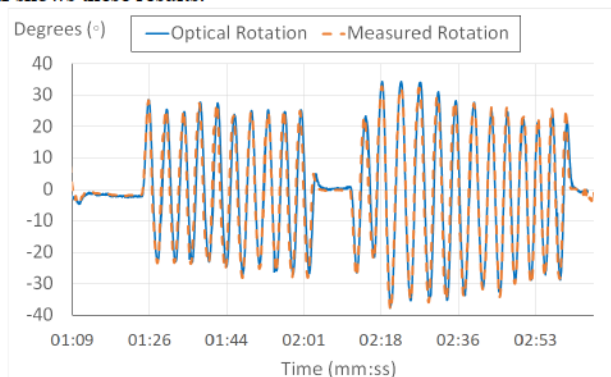


Fig. 8. Example of bend rotation measured by the device and by the optical system in the thoracic sensor, for a segment with two series of exercises extracted from one of the recording sessions from the validation experiments.

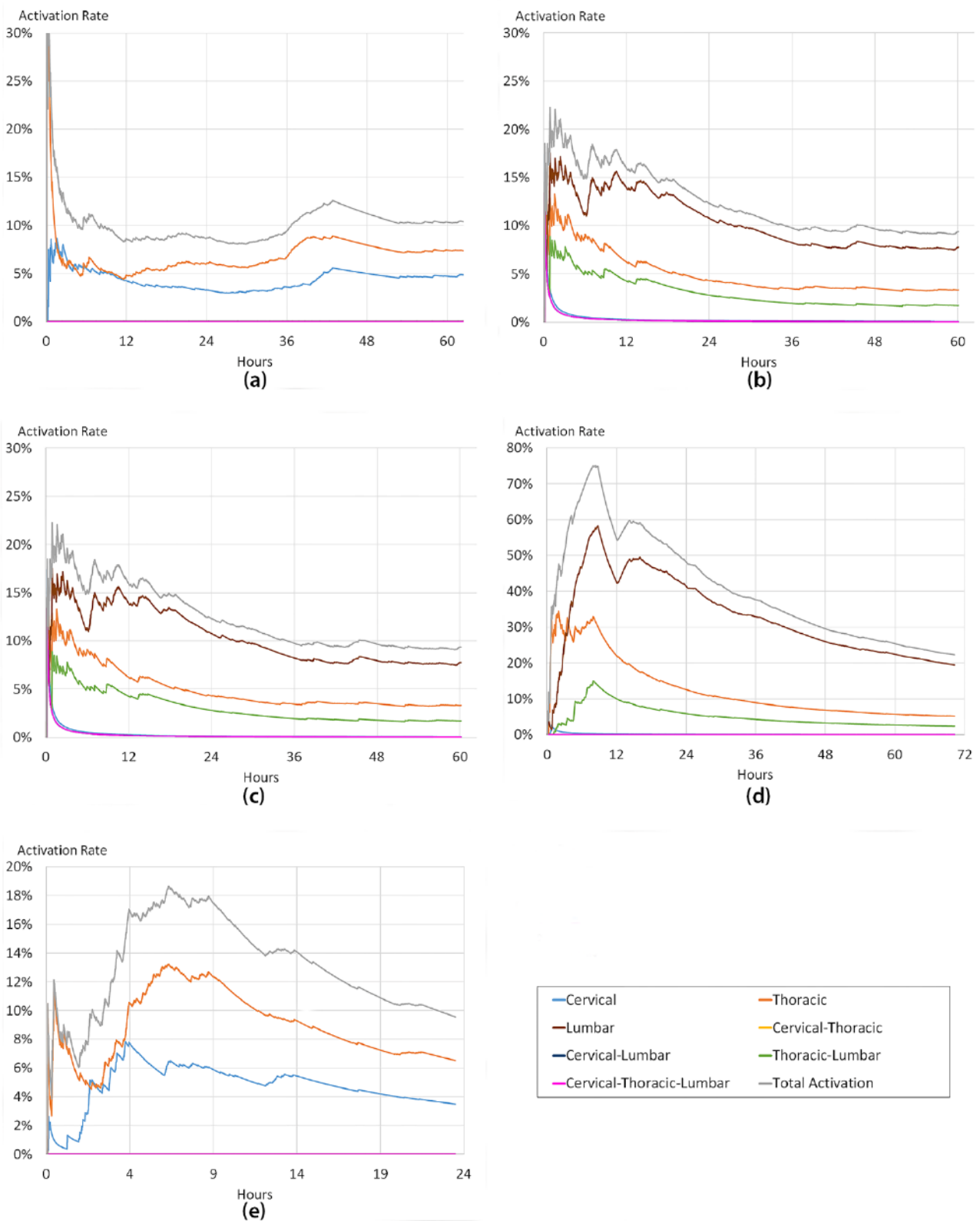


Fig. 9. Results of the pilot study performed at the Spinal Cord Injury Unit of the University Hospital Complex of A Coruña, Spain. With patients afflicted by *lumbar hyperlordosis* or *lumbar hypolordosis* 1 (a) to 5 (e). The plots show the evolution of the absolute and relative activation rates of the sensors of the wearable device. These activation rates indicate the percentage of time leaning forward or backward in an incorrect way.

TABLE III
AVERAGE ERROR (°)

Work	RMS Deviation
Wong and Wong, 2008 [18]	≤ 1.50
Wong and Wong, 2009 [17]	≤ 3.10
Mjøsund et al., 2017 [16]	≤ 1.80
This work	≤ 1.24

D. Clinical pilot study

To verify the suitability of the system in a clinical scenario with a set of trials with five patients affected with low back pain and needing postural therapy performed at the Spinal Cord Injury Unit of the University Hospital Complex of A Coruña, Spain.

Inclusion criteria for our study included all adult patients (ages from 18 to 65) afflicted by *lumbar hyperlordosis* or *lumbar hypolordosis* who underwent a back school program with lessons given by a therapist with the aim of preventing low back pain.

The five selected patients had the same gender and profession, and no patient was excluded from the study.

Before the experiment, all patients answered a quality of life assessment survey that included a Visual Analog Scale (VAS) about back pain. The VAS scale used for this study measures from 0-10 the intensity of the pain where 0 represents no pain and 10 represents the worst possible pain.

After an initial assessing, the clinician configured the device with the physiological characteristics of each patient; and introduced the patient to the device and the protocol. Each patient then wore the device during normal daily activities, such as working in a computer in an office chair, in 10 to 35 sessions in a period of 4 months. Each session had a minimum duration of one hour, depending on the evolution and availability of each patient, no patient reported discomfort or pain during the exercises.

The experiment was limited to monitoring the anomalies in the Y-axis (*Tilt*), i.e. leaning forward or backward in an incorrect way. Since only this movement was relevant for the clinicians in relation with the conditions of *lumbar hyperlordosis* or *lumbar hypolordosis*. Fig. 9 shows the obtained results.

After the experiment, all patients underwent a clinical analysis and answered the survey again. In all patients, we observed an improvement in the reaction time to the stimulus, the clinical analysis reported an improved postural control after a small number of sessions and all patients reported an improvement in quality of life and a reduction of low back pain of 2 points in average in the VAS scale.

These results show a very promising potential for learning postural control in therapy environments for low back pain. However, more experiments with bigger sample sizes, and stronger experimental controls are required in order to obtain meaningful statistical results.

The device is now undergoing additional test, and more clinical trials are being planned in different centers of different nations.

E. Cost Comparison

As far as our knowledge goes, none of the authors in the literature made their prototype available to the public or provided a price estimation. Table IV shows a prize comparison of available commercial alternatives with the price of our device if developed commercially, according to our estimations. We included all products that to our knowledge can be used to monitor the posture of the back, and no product was excluded.

TABLE IV
PRIZE COMPARISSION

Product	Prize
Lumo Fit [35]	Discontinued
Valedo Motion [36]	3,930.00\$*
ViMove2 [37]	1,990.00\$ / 149.00\$ month**
This work	≤ 100\$

*Prize from authorized federal supply schedule price list [48].

**Monthly subscription includes free access to the myViMove patient application.

IV. CONCLUSION

We designed a non-invasive, cost effective wearable device to measure the back position, study spinal deviations and establish a control method that helps individuals to control their posture; with the aim of improving the effectiveness of physical therapies in low back pain patients.

This device uses gyroscopes, accelerometers and magnetometers to measure the angular movements in different sections of the back, and performs an integrated analysis to obtain the postural information of the patient in real time.

The device uses a fuzzy expert system to send a physiological “feedback” to the patient. This signal is a vibration that communicates that the current posture deviates from the parameters estimated by the clinician and needs a correction, as far as we know, this is the first time this approach is used in a control system for low back pain therapy.

We validated the device in laboratory and real conditions, improving previous results and showing that our device reliably measures the correct and incorrect postural situation of the spine in each of its sections, and as a whole.

We tested the device in a clinical pilot study with 5 patients. In all cases an improved postural control, an improvement in quality of life and a reduction of low back pain were observed. Also none of the patients reported discomfort or pain in the training sessions in the 4 months of the pilot study. These results, indicate that a wearable system such as the one we present will be useful in therapy to increase posture control, reduce low back pain, perform back exercises in a more effective way, and to increase posture awareness in patients. This is, as far as we know, the first time a postural control system reports results with low back pain patients.

According to our estimations this device could be made available for purchase with a cost below 100\$, an order of magnitude below the cost of current commercial solutions. And we plan to release a version of the prototype in that prize range.

AUTHOR CONTRIBUTIONS

Alvaro Rodriguez wrote the manuscript, conducted the validation experiments, analyzed all the data and elaborated the original figures; Juan R. Rabuñal designed the device and developed the prototype; Antonio Rodríguez Sotillo conducted the clinical pilot study; Alejandro Pazos and Norberto Ezquerria supervised the clinical results. All authors revised and edited the manuscript.

ACKNOWLEDGMENT

We would like to thank the BioBack platform and Jose Cuevas from Tecnofor Puerto Rico, for their support in the development of the device; and the PhD student Martín Nogueira for his initial collaboration in the project.

This work was supported by the funding of the unique installation BIOCAI (UNLC08-1E-002, UNLC13-13-3503) and the European Regional Development Funds (FEDER) by the European Union.

Additional support was offered by the Consolidation and Structuring of Competitive Research Units—Competitive Reference Groups (ED431C 2018/49) and Accreditation, Structuring, and Improvement of Consolidated Research Units and Singular Centers (ED431G/01), funded by the Ministry of Education, University and Vocational Training of the Xunta de Galicia endowed with EU FEDER funds.

REFERENCES

- [1] K. Walsh, N. Varnes, C. Osmond, R. Styles, and D. Coggon, "Occupational causes of low-back pain," *Scand. J. Work Environ. Health*, pp. 54–59, 1989.
- [2] J. K. Freburger *et al.*, "The rising prevalence of chronic low back pain," *Arch. Intern. Med.*, vol. 169, no. 3, pp. 251–258, 2009.
- [3] R. A. Deyo, J. Rainville, and D. L. Kent, "What can the history and physical examination tell us about low back pain?," *Jama*, vol. 268, no. 6, pp. 760–765, 1992.
- [4] B. W. Koes, M. W. Van Tulder, and S. Thomas, "Diagnosis and treatment of low back pain," *Bmj*, vol. 332, no. 7555, pp. 1430–1434, 2006.
- [5] S. M. Rubinstein, A. De Zoete, M. Van Middelkoop, W. J. J. Assendelft, M. R. De Boer, and M. W. Van Tulder, "Benefits and harms of spinal manipulative therapy for the treatment of chronic low back pain: systematic review and meta-analysis of randomised controlled trials," *bmj*, vol. 364, p. 1689, 2019.
- [6] D. Steffens *et al.*, "Prevention of low back pain: a systematic review and meta-analysis," *JAMA Intern. Med.*, vol. 176, no. 2, pp. 199–208, 2016.
- [7] H. M. School, "Posture and back health," *Harvard Medical Publishing*, 2014. <https://www.health.harvard.edu/pain/posture-and-back-health> (accessed Feb. 08, 2020).
- [8] V. Leinonen *et al.*, "Lumbar paraspinal muscle function, perception of lumbar position, and postural control in disc herniation-related back pain," *Spine (Phila. Pa. 1976)*, vol. 28, no. 8, pp. 842–848, 2003.
- [9] K. Claeys, S. Brumagne, W. Dankaerts, H. Kiers, and L. Janssens, "Decreased variability in postural control strategies in young people with non-specific low back pain is associated with altered proprioceptive reweighting," *Eur. J. Appl. Physiol.*, vol. 111, no. 1, pp. 115–123, 2011.
- [10] C. Costa, D. Tacconi, R. Tomasi, F. Calva, and V. Terreri, "RIABLO: a game system for supporting orthopedic rehabilitation," in *Proceedings of the Biannual Conference of the Italian Chapter of SIGCHI*, 2013, pp. 1–7.
- [11] S. Saponara, "Wearable biometric performance measurement system for combat sports," *IEEE Trans. Instrum. Meas.*, vol. 66, no. 10, pp. 2545–2555, 2017.
- [12] B. Andò *et al.*, "A measurement system to monitor postural behaviour: strategy assessment and classification rating," *IEEE Trans. Instrum. Meas.*, 2020.
- [13] G. M. Bertolotti *et al.*, "A wearable and modular inertial unit for measuring limb movements and balance control abilities," *IEEE Sens. J.*, vol. 16, no. 3, pp. 790–797, 2015.
- [14] B.-C. Lee, S. Chen, and K. H. Sienko, "A wearable device for real-time motion error detection and vibrotactile instructional cuing," *IEEE Trans. Neural Syst. Rehabil. Eng.*, vol. 19, no. 4, pp. 374–381, 2011.
- [15] A. Fathi and K. Curran, "Detection of spine curvature using wireless sensors," *J. King Saud Univ.*, vol. 29, no. 4, pp. 553–560, 2017.
- [16] H. L. Mjøsund, E. Boyle, P. Kjaer, R. M. Mieritz, T. Skallgård, and P. Kent, "Clinically acceptable agreement between the ViMove wireless motion sensor system and the Vicon motion capture system when measuring lumbar region inclination motion in the sagittal and coronal planes," *BMC Musculoskelet. Disord.*, vol. 18, no. 1, pp. 1–9, 2017.
- [17] W.-Y. Wong and M.-S. Wong, "Measurement of postural change in trunk movements using three sensor modules," *IEEE Trans. Instrum. Meas.*, vol. 58, no. 8, pp. 2737–2742, 2009.
- [18] W. Y. Wong and M. S. Wong, "Smart garment for trunk posture monitoring: A preliminary study," *Scoliosis*, vol. 3, no. 1, p. 7, 2008.
- [19] M. Bazzarelli, N. G. Durdle, E. Lou, and V. J. Raso, "A wearable computer for physiotherapeutic scoliosis treatment," *IEEE Trans. Instrum. Meas.*, vol. 52, no. 1, pp. 126–129, 2003.
- [20] N. Mijailović, A. Peulić, N. Filipović, and E. Jovanov, "Implementation of wireless sensor system in rehabilitation after back spine surgery," *Serbian J. Electr. Eng.*, vol. 9, no. 1, pp. 63–70, 2012.
- [21] E. Sardini, M. Serpelloni, and V. Pasqui, "Wireless wearable T-shirt for posture monitoring during rehabilitation exercises," *IEEE Trans. Instrum. Meas.*, vol. 64, no. 2, pp. 439–448, 2014.
- [22] E. Sardini, M. Serpelloni, and V. Pasqui, "Daylong sitting posture measurement with a new wearable system for at home body movement monitoring," in *2015 IEEE International Instrumentation and Measurement Technology Conference (I2MTC) Proceedings*, 2015, pp. 652–657.
- [23] M. G. Benedetti, F. Biagi, A. Merlo, C. Belvedere, and A. Leardini, "A new protocol for multi-segment trunk kinematics," in *2011 IEEE International Symposium on Medical Measurements and Applications*, 2011, pp. 442–445.
- [24] L. E. Dunne, P. Walsh, B. Smyth, and B. Caulfield, "Design and evaluation of a wearable optical sensor for monitoring seated spinal posture," in *2006 10th IEEE International Symposium on Wearable Computers*, 2006, pp. 65–68.
- [25] G. Baroni, C. Rigotti, A. Amir, G. Ferrigno, D. Newman, and A. Pedotti, "Multifactorial movement analysis in weightlessness: a ground-based feasibility study," *IEEE Trans. Instrum. Meas.*, vol. 49, no. 3, pp. 476–482, 2000.
- [26] A. Maduri and S. E. Wilson, "Lumbar position sense with extreme lumbar angle," *J. Electromyogr. Kinesiol.*, vol. 19, no. 4, pp. 607–613, 2009.
- [27] A. P. Claus, J. A. Hides, G. L. Moseley, and P. W. Hodges, "Is 'ideal' sitting posture real?: Measurement of spinal curves in four sitting postures," *Man. Ther.*, vol. 14, no. 4, pp. 404–408, 2009.
- [28] O. A. Postolache, P. M. B. S. Girao, J. Mendes, E. C. Pinheiro, and G. Postolache, "Physiological parameters measurement based on wheelchair embedded sensors and advanced signal processing," *IEEE Trans. Instrum. Meas.*, vol. 59, no. 10, pp. 2564–2574, 2010.
- [29] J. Baek and B.-J. Yun, "Posture monitoring system for context awareness in mobile computing," *IEEE Trans. Instrum. Meas.*, vol. 59, no. 6, pp. 1589–1599, 2010.
- [30] G.-D. Voinea, S. Butnariu, and G. Mogan, "Measurement and geometric modelling of human spine posture for medical rehabilitation purposes using a wearable monitoring system based on inertial sensors," *Sensors*, vol. 17, no. 1, p. 3, 2017.
- [31] O. Dehzaangi, Z. Zhao, M.-M. Bidmeshki, J. Biggan, C. Ray, and R. Jafari, "The impact of vibrotactile biofeedback on the excessive walking sway and the postural control in elderly," in *Proceedings of the 4th Conference on Wireless Health*, 2013, p. 3.
- [32] A. Tino, M. Carvalho, N. F. Preto, and K. M. V. McConville, "Wireless vibrotactile feedback system for postural response improvement," in *2011 Annual International Conference of the IEEE Engineering in Medicine and Biology Society*, 2011,

- pp. 5203–5206.
- [33] M. Eid, U. Saad, and U. Afzal, “A real time vibrotactile biofeedback system for optimizing athlete training,” in *2013 IEEE International Symposium on Haptic Audio Visual Environments and Games (HAVE)*, 2013, pp. 1–6.
- [34] M. R. Afzal, M.-K. Oh, C.-H. Lee, Y. S. Park, and J. Yoon, “A portable gait asymmetry rehabilitation system for individuals with stroke using a vibrotactile feedback,” *Biomed Res. Int.*, vol. 2015, 2015.
- [35] Lumo, “Lumo Fit.” <https://www.lumobodytech.com/lumo-lift/>.
- [36] Hocoma, “Valedo Motion.” <https://www.hocoma.com/solutions/valedo-motion/>.
- [37] Dorsavi, “ViMove2.” <https://www.dorsavi.com/au/en/vimovestore/>.
- [38] P. D. Groves, “Principles of GNSS, inertial, and multisensor integrated navigation systems, 2nd edition [Book review],” *IEEE Aerospace and Electronic Systems Magazine*, vol. 30, no. 2, pp. 26–27, 2015, doi: 10.1109/MAES.2014.14110.
- [39] O. J. Woodman, “Introduction to Inertial Navigation,” Computer Laboratory, University of Cambridge, 2007. doi: 10.1017/S0373463300036341.
- [40] A. Figuero, A. Rodriguez, J. Sande, E. Peña, and J. R. Rabuñal, “Field measurements of angular motions of a vessel at berth: Inertial device application,” 2018.
- [41] W. Premerlani and P. Bizard, “Direction cosine matrix imu: Theory,” *DIY Drones*, 2009, [Online]. Available: <http://robot-chopper.googlecode.com/svn/trunk/Research/DCMDraft2.pdf>.
- [42] J. G. Ziegler and N. B. Nichols, “Optimum Settings for Automatic Controllers,” *Transaction of the A.S.M.E.*, vol. 64, pp. 759–768, 1942, doi: 10.1115/1.2899060.
- [43] A. Figuero, A. Rodriguez, J. Sande, E. Peña, and J. R. Rabuñal, “Dynamical Study of a Moored Vessel Using Computer Vision,” *J. Mar. Sci. Technol.*, vol. 26, no. 2, pp. 240–250, 2018, doi: 10.6119/JMST.2018.04_(2).0011.
- [44] A. Rodriguez, “A methodology to develop Computer Vision systems in Civil Engineering: Applications in material testing and fish tracking,” University of A Coruña (Doctoral dissertation), 2014.
- [45] OpenCV Developers Team, “Open source computer vision library.” <http://opencv.org>, 2016.
- [46] A. Rodriguez, C. Fernandez-Lozano, J. Dorado, and J. R. Rabuñal, “Two-dimensional gel electrophoresis image registration using block-matching techniques and deformation models,” *Anal. Biochem.*, vol. 454, no. 0, pp. 53–59, 2014, doi: <http://dx.doi.org/10.1016/j.ab.2014.02.027>.
- [47] A. Rodriguez, J. R. Rabuñal, J. L. Pérez, and F. Martínez-Abella, “Optical Analysis of Strength Tests Based on Block-Matching Techniques,” *Comput. Civ. Infrastruct. Eng.*, vol. 27, no. 8, pp. 573–593, Sep. 2012, doi: 10.1111/j.1467-8667.2011.00743.x.
- [48] Dep. Veterans Affairs, “Authorized Federal Supply Schedule Price List,” 2020. https://www.gsaadvantage.gov/ref_text/V797P4377B/0LHJK8.2LAVSP_V797P-4377B_GYNDISPTEXTFILE.PDF.